IEEJ Journal of Industry Applications
Vol.7 No.6 pp.488–494 DOI: 10.1541/ieejjia.7.488

Paper

Dual-loop Controller Design Considering Robust Vibration Suppression in Piezo-actuated Stage Systems

Kenta Seki[*a)] Senior Member, Daisuke Noda[*] Member
Makoto Iwasaki[*] Senior Member

(Manuscript received Jan. 10, 2018, revised June 6, 2018)

This paper presents a controller design approach considering robust vibration suppression against resonant frequency variations in piezo-actuated systems. In piezo-actuated systems, the improvement of suppression performance with respect to external disturbances and nonlinearities such as hysteresis and creep by the expansion of feedback control bandwidth is indispensable for achieving high-precision positioning. The vibration suppression approach is a key technology for the expansion of bandwidth. From a practical point of view, a minor feedback loop including a simple compensator with a few parameters to increase the design freedom is added to the general feedback control system. In the minor-loop design, the reduction of sensitivity gain at around the resonant frequencies is considered to suppress the residual vibration of the references and disturbances, and the loop-shaping approach based on the frequency domain is adopted to provide an intuitive and practical design guideline. A major-loop for an augmented plant, including the minor-loop, is designed by considering the system stability, servo bandwidth, and settling performance. The proposed approach is verified by conducting experiments using a commercial piezo-actuated stage system.

Keywords: high-precision positioning, vibration suppression, loop-shaping, robust property, piezo-actuated stages

1. Introduction

High-precision positioning is one of key technologies in various mechatronic products such as storage devices [(1)–(3)], industrial machines [(4)(5)], and manipulators [(6)–(8)]. As one of the actuator devices in the mechatronic systems, piezoelectric actuators have been widely used in nanopositioning fields, e.g., nanopositioning stage systems, nanorobotic manipulators, and scanning probe microscopes (SPMs) such as scanning tunneling microscopes (STMs) and atomic force microscopes (AFMs), because of the advantages of high resolution, rapid response, non-magnetic field, and large force generation for the volume [(9)]. However, the piezo-actuated systems generally include uncertainties such as nonlinearities due to hysteresis and creep phenomena, which deteriorate the positioning and/or tracking accuracy. In addition, resonant vibrations in the mechanism lead to vibratory responses or system instability. In order to achieve the higher precise control performance, therefore, it is necessary to compensate for the nonlinear characteristics as well as mechanical resonant vibrations.

Hysteresis is one of the typical nonlinear characteristics in the piezoelectric actuators, which appears between the applied voltage and the output displacement. In the open-loop control, various types of modeling and the inverse model-based feedforward compensation approaches for the hysteresis have been proposed, e.g., the Bouc-Wen model-based compensation [(10)], the Preisach model-based compensation [(11)], and the Prandtl-Ishlinskii model-based compensation [(12)]. However, the drawback is the substantial modeling complexity and time-consuming modeling process because of the difficulties in understanding the hysteresis behavior and deriving complex mathematical models for the same. In addition, although the inverse model-based approach is one of powerful tools to completely compensate for the hysteresis, the compensation performance depends on the accuracy of the modeling. As a result, the control performance is unsatisfactory because of modeling error and/or parameter variations. The creep phenomenon, which is another nonlinear component, requires complex mathematical modeling and parameter tuning, where the problem associated with the hysteresis compensation exists in the open-loop control.

Feedback control systems using high-resolution sensors are indispensable to overcome the problem of the open-loop control [(13)]. In the feedback control systems, the improvement of sensitivity characteristic by high gain feedback controller is required to suppress the nonlinearities and other disturbances [(14)]. However, the feedback gain cannot be adequately increased because the general positioning mechanisms that employ piezoelectric actuators inherently include mechanical vibration modes. In addition, the mechanical resonant frequencies become lower because the piezo-actuated systems are generally applied the flexure hinge mechanisms to enlarge the output displacement [(15)]. The vibrational dynamics tend to have a low stability margin because of the sharp resonant peaks associated with the low structural damping. Although notch filters or state feedback are practically used to suppress

a) Correspondence to: Kenta Seki. E-mail: k-seki@nitech.ac.jp
* Department of Electrical and Mechanical Engineering, Nagoya Institute of Technology
Gokiso, Showa-ku, Nagoya, Aichi 466-8555, Japan

the resonant peaks as studied in Refs. (13), (16), (17), it is difficult to ensure the robust stability against resonant frequency variations. In addition, the phase delay in the notch filters decreases the phase margin. Feedforward approaches [18] using inverse dynamics of mechanical resonances cannot suppress the resonant vibrations for the input disturbances as well as low robustness of suppression performance. Passive/active damping techniques without additional sensors are proposed to increase the effective structural damping for the piezo-actuated systems [19][20]. Although these approaches can give damping effect to the existing system using shunt or bridge circuit, these external circuits are difficult to tune the optimal parameters using analog devices. In addition, sufficient damping effect cannot be obtained because detection signal through the circuit is very small. In Ref. (21), vibration suppression of piezo-actuated system was achieved using dual-sensor. However, the additional sensor leads to an increase in cost, and the commercial products may be difficult to add the new sensors. As other approaches, on the other hand, advanced control techniques have been developed to improve the control accuracy and bandwidth, e.g., adaptive methods [22], robust control approach [23], sliding mode control [24], and repetitive control [25]. However, these control techniques cannot be implemented in some cases, e.g., high computational cost, complex algorithms, and difficult parameter tuning process. Therefore, these approaches should be appropriately selected considering the control purpose, plant characteristics, computational performance of the controller, sensor resolution, etc. In addition, from the practical point of view, the control structure and the design guideline should be simplicity and clear.

As a new approach, this paper presents a design approach to achieve robust vibration suppression against resonant frequency variations without additional sensors and low computational cost in the piezo-actuated systems, where the goal is to achieve the control purpose by a simple control structure under the use of single sensor. In this approach, minor feedback loop including a simple compensator is added on the general feedback control system to increase the design freedom because simple feedback control structure is difficult to satisfy some control purposes simultaneously. From the practical point of view, control structure of additional loop is considered simplicity of design and ease of parameter tuning. The design of minor-loop only focuses on the suppression of resonant vibration modes, where the reduction of sensitivity characteristic at around the resonant frequencies is especially considered to attenuate the residual vibration for the references and disturbances. The loop-shaping approach [26][27] based on the frequency domain is adopted to provide the intuitive and practical design guideline. Major-loop for an augmented plant including the minor-loop, on the other hand, is designed by considering the system stability, servo bandwidth, and settling performance. The effectiveness of proposed design approach is verified by conducting experiments using a commercial piezo-actuated stage system.

2. System Configuration and Plant Model

2.1 System Configuration of Target Piezo-actuated Stage System Figure 1 shows an overview of target piezo-actuated stage with a high resolution capacitive

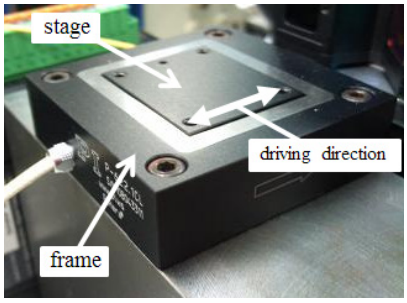

Fig. 1. Overview of target piezo-actuated stage

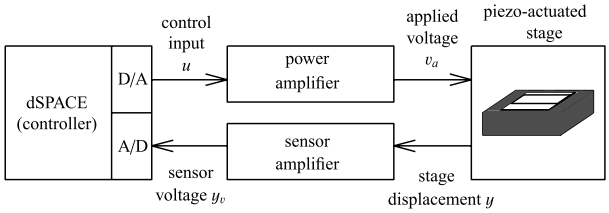

Fig. 2. System configuration of piezo-actuated stage

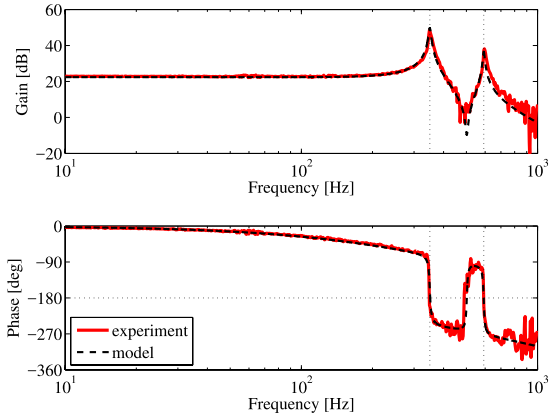

Fig. 3. Frequency characteristics of sensor voltage y_v for control input u

position sensor (P-622.1, Physik Instrumente GmbH & Co. KG.) as an experimental setup. The stage (25 [mm] × 30 [mm]) is constrained to move only in one direction with the help of frictionless elastic hinges. The maximum stroke of stage is 250 [μm], which is obtained using the integrated displacement amplifier mechanisms. Figure 2 shows the system configuration as the experimental setup. The stage position y is detected using the capacitive sensor in the frame part of the stage system. The stage position is transferred to a controller board (DS1103, dSPACE GmbH) through an sensor amplifier (E-610, Physik Instrumente GmbH & Co. KG.) with a sampling period of 0.1 [ms]. A stacked piezoelectric actuator is driven based on the control input u through a power amplifier (HSA 4014, NF Corporation). The gain of power amplifier is set as 10.

2.2 Model of Plant Characteristic The solid red lines in Fig. 3 show the frequency characteristic of the sensor voltage y_v for the control input u. The characteristic is measured using a dynamic signal analyzer (35670 A, Agilent Technologies, Inc.) by employing swept-sine excitations. The figure shows that the mechanism includes two mechanical vibration modes due to the elastic deformation of the hinges in the high frequency range. Therefore, a mechanical

Table 1. Parameters of plant model

ω_{m1} [rad/s]	$2\pi\times$ 354	ζ_{m1}	0.012	k_{m1}	4.02
ω_{m2} [rad/s]	$2\pi\times$ 592	ζ_{m2}	0.015	k_{m2}	3.29
K_a	10.0	K_g	4.8×10^4	K_c	25.0
ω_c [rad/s]	$2\pi\times$ 240	L_c [μs]	120		

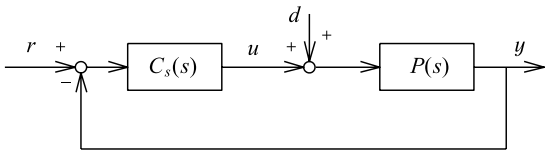

Fig. 4. Block diagram of simple feedback control system

part as the linear dynamics can be formulated as a plant mathematical model $P(s)$, which comprises two vibration modes and a dead time component:

$$P(s) = \frac{y_v}{u} = K_a P_m(s) P_c(s), \quad \cdots\cdots (1)$$

$$P_m(s) = \frac{y}{v_a} = K_g \left(\sum_{i=1}^{2} \frac{k_{mi}}{s^2 + 2\zeta_{mi}\omega_{mi} s + \omega_{mi}^2} \right), \quad \cdots\cdots (2)$$

$$P_c(s) = \frac{y_v}{y} = K_c \frac{\omega_c}{s + \omega_c} e^{-L_c s}, \quad \cdots\cdots (3)$$

where K_a: gain of power amplifier, K_g: linear plant gain, K_c: gain of sensor amplifier, ω_{mi}: natural angular frequency of ith vibration mode, ζ_{mi}: damping coefficient of ith vibration mode, k_{mi}: modal constant of ith vibration mode, ω_c: cutoff frequency of lowpass filter in the sensor amplifier, and L_c: equivalent dead time, respectively. As the cutoff frequency of the power amplifier is above 10 [kHz], the characteristic is considered as a gain component. The broken lines in Fig. 3 show the frequency characteristic of the mathematical model $P(s)$. Table 1 lists the model parameters identified via curve-fitting.

2.3 Simple Feedback Control System In general, a simple feedback control system shown in Fig. 4 is designed for the plant $P(s)$. In the figure, $C_s(s)$ indicates the feedback compensator, r indicates the position reference, and d indicates the input disturbance. From Fig. 3, each vibration mode has sharp peaks. The gain peak of the 1st resonant frequency is approximately 30 [dB] higher than the DC gain of the plant. In the feedback controller design, therefore, damping should be sufficient to ensure the stability of the system and avoidance of the residual vibrations. As a simple approach to compensate for the effects of the vibration modes using a feedback compensator, gain compensation using the notch filters is practically applied in the industrial products. On the other hand, phase-stabilized design using a vector locus of an open-loop characteristic has been proposed, where the circular vector locus of the vibration modes expands far away from the (−1, 0) on the Nyquist plot [26]. Here, Fig. 5 shows the vector locus of the plant characteristic. The figure shows that the vector loci of each vibration mode draw the left-side on the complex plane. In addition, these vibration modes are in-phase mode. In the design of feedback compensator, therefore, not the phase-stabilized design but the gain compensation approach should be applied to compensate for these vibration modes.

On the basis of the design guideline for the vibration suppression, the feedback compensator $C_s(s)$ should include two

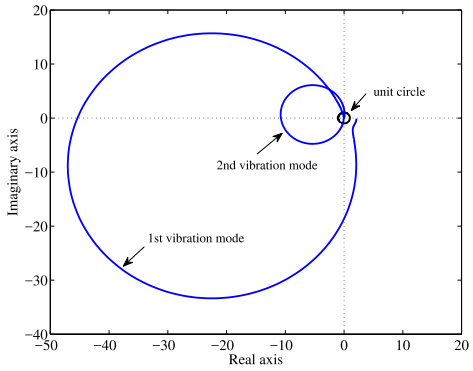

Fig. 5. Vector locus of plant characteristic

Table 2. Parameters of $C_s(s)$

K_{P1}	0.0113	K_{I1}	7.93		
ω_{c1}[rad/s]	$2\pi\times354$	ζ_{cn1}	0.01	ζ_{cd1}	1.0
ω_{c2}[rad/s]	$2\pi\times592$	ζ_{cn2}	0.01	ζ_{cd2}	1.0

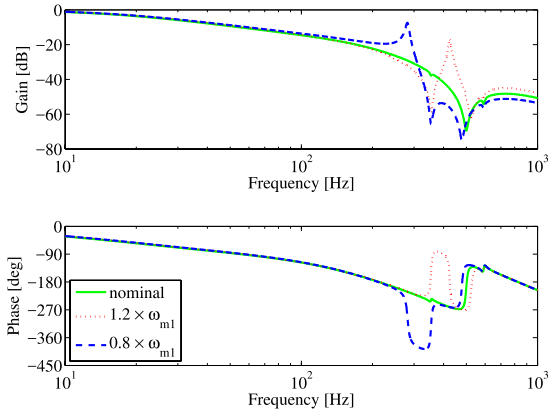

Fig. 6. Closed-loop characteristics of gain compensation by notch filters

notch filters to reduce the gain peaks at resonant frequencies. In addition, an integral compensation is required for $C_s(s)$ to improve the steady state performance for the step reference. From the above points, $C_s(s)$ is designed as follows.

$$C_s(s) = \left(K_{P1} + \frac{K_{I1}}{s} \right) \cdot \prod_{i=1}^{2} \frac{s^2 + 2\zeta_{cni}\omega_{ci} + \omega_{ci}^2}{s^2 + 2\zeta_{cdi}\omega_{ci} + \omega_{ci}^2} \cdots\cdots (4)$$

Table 2 lists the designed parameters of $C_s(s)$. These parameters are tuned by considering the stability of the system and settling performance without residual vibration. Figure 6 shows closed-loop characteristics of y for r in Fig. 4, where the solid green lines indicate the characteristic under nominal condition without resonant frequency variations, the dotted red lines indicate the characteristic for the 1st resonant frequency variation of +20% (it means $1.2\times\omega_{m1}$), and the broken blue lines indicate the characteristic for the 1st resonant frequency variation of −20% (it means $0.8\times\omega_{m1}$). From this figure, the suppression performance against the variations in the resonant frequency is insufficient. In addition, the resonant vibrations are excited by the input disturbance d in the feedback control system of Fig. 4 because the gain peaks of each vibration mode are approximately 40 [dB]. Therefore, the application of other compensation approach is indispensable for this plant to achieve the high performance of

vibration suppression and the robust property against resonant frequency variations.

3. Design of Feedback Control System with Minor-loop

3.1 Design Guideline An additional compensator should be introduced to achieve the several requirements for the control system of the target piezo-actuated stage system because it is difficult to achieve the robust vibration suppression against resonant frequency variations by a single feedback compensator. In addition, it is necessary to give a clear design guideline for each compensator.

Figure 7 shows the feedback control system with minor-loop. In this control system, minor-loop focuses on the robust compensation for the vibration modes with frequency vibrations. Thus, the minor-loop compensator $C_1(s)$ is designed considering the reduction of the sensitivity gain at around the resonant frequencies in the minor-loop. On the other hand, the design of major-loop is only considered for the simple plant characteristic without vibration modes because the gain peaks at resonant frequencies are attenuated by the minor-loop. The compensator $C_2(s)$ is designed considering system stability, servo bandwidth, and settling performance. The design guideline and parameter tuning of each compensator becomes clear by adding the minor-loop.

3.2 Minor-loop Controller Design From the viewpoint of phase stabilization design for the resonant vibrations, vector loci should be drawn in the right side on the complex plane in order to reduce the sensitivity gains at the resonant frequencies. The phase at 1st resonant frequency 354 [Hz] is approximately −170 [deg] from the plant characteristic shown in Fig. 3. Therefore, negative term should be included to change the phase 180 [deg] in $C_1(s)$. In addition, the lowpass filter is designed to adjust the phase at resonant frequencies and to avoid spillover in the high frequency. From the above design guideline, $C_1(s)$ is given as

$$C_1(s) = \frac{-K_{mc}\omega_{mc}}{s + \omega_{mc}}. \quad \cdots\cdots (5)$$

Table 3 lists the designed parameters of $C_1(s)$, where these parameters are tuned based on the vector loci of minor-loop. Figure 8 shows the Nyquist diagrams. Figure 9 shows the sensitivity gains (u/u') and the gain characteristics (y/u') of minor-loop. In these figures, solid lines indicate the characteristic under the nominal condition without the resonant frequency variation, broken lines indicate the characteristic under 1st resonant frequency variation of +20% ($1.2\times\omega_{m1}$), and dotted lines indicate the characteristic under 1st resonant frequency variation of −20% ($0.8\times\omega_{m1}$). From Fig. 8, vector loci of vibration modes are drawn in the right side on the complex plane. As a result, the sensitivity gains and gain peaks of minor-loop characteristic (y/u') can be reduced under the frequency variations.

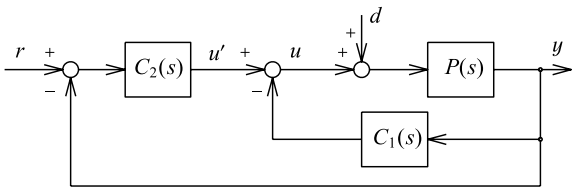

Fig. 7. Feedback control system with minor-loop

Table 3. Parameters of each compensator

$C_1(s)$			
K_{mc}	0.024	ω_{mc}	$2\pi\times 1000$
$C_2(s)$			
K_P	2.7×10^{-3}	K_I	4.2

This minor-loop compensator only has two parameters. In addition, these parameters can be intuitively designed on the frequency domain. These points are a big advantage in the industrial application. Moreover, it is possible to avoid the spillover for unknown vibration modes in the high frequency range because the minor-loop compensator is composed by lowpass filter.

3.3 Major-loop Controller Design The major-loop feedback compensator $C_2(s)$ is designed for the augmented plant including minor-loop. Here, since the vibration modes in the plant are sufficiently compensated by the minor-loop, design of $C_2(s)$ is only considered the system stability, the servo bandwidth, and the settling performance for the simple plant without vibration modes. In this article, a simple Proportional-Integral (PI) compensator is designed as follows:

$$C_2(s) = K_P + \frac{K_I}{s}. \quad \cdots\cdots (6)$$

Table 3 lists the designed parameters, where the parameters are especially tuned by considering the settling performance.

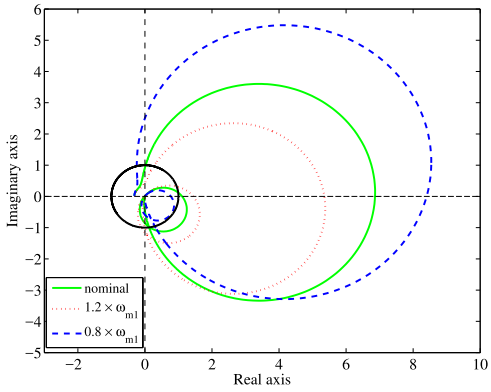

Fig. 8. Nyquist diagrams of minor-loop

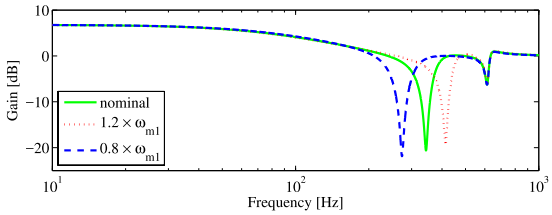

(a) sensitivity gains of minor-loop (u/u').

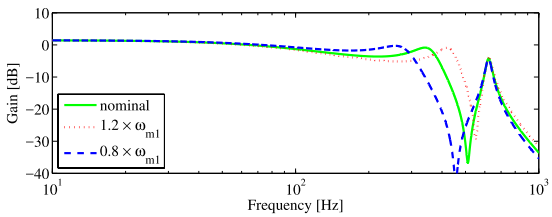

(b) gain characteristics of minor-loop (y/u')

Fig. 9. Minor-loop characteristics

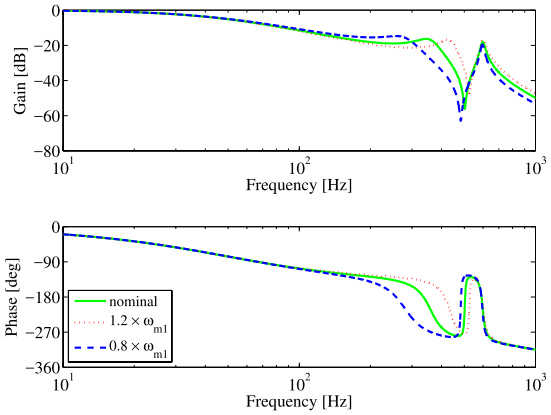

Fig. 10. Closed-loop characteristics of major-loop (y/r)

Figure 10 shows the closed-loop characteristics (y/r). From the figure, robust vibration suppression against frequency variations can be achieved by applying the minor-loop compensation.

4. Experimental Verifications

Effectiveness of the proposed approach is verified by conducting experiments using the piezo-actuated stage system shown in Fig. 2. In the experiments, the resonant frequency variation is simulated by placing a load on the stage to verify the robust vibration suppression performance. The broken lines in Fig. 11 show the plant characteristic with a load of 22 [g] acting on the stage, while the solid lines indicate the nominal plant characteristic shown in Fig. 3. This result shows that the 1st resonant frequency changes to 290 [Hz] (−64 [Hz]) after placing the load.

Figure 12 shows the displacement reference in the inching motion for an amplitude interval of 40 [μm], and Fig. 13 shows the displacement reference in the step motion with different amplitudes. Figures 14 and 15 show the error waveforms between the reference and the response, where (a) indicates the results for the single-loop control system with notch filters shown in Fig. 4 and (b) indicates the results for the dual-loop control system shown in Fig. 7. In each error waveform, the magnified error waveforms represent the step-reference input time of 0 [s]. This result confirms that the residual vibration after positioning for each response can be suppressed using the dual-loop control system. The maxi-

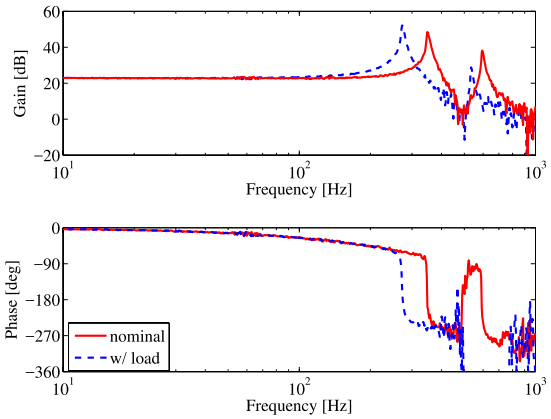

Fig. 11. Frequency characteristics of plant with load

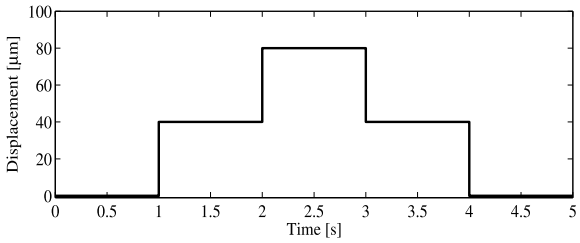

Fig. 12. Position reference in inching motion

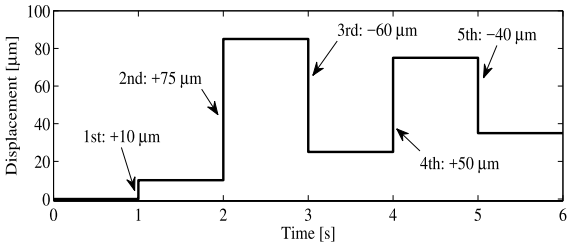

Fig. 13. Position reference in step motion with different amplitudes

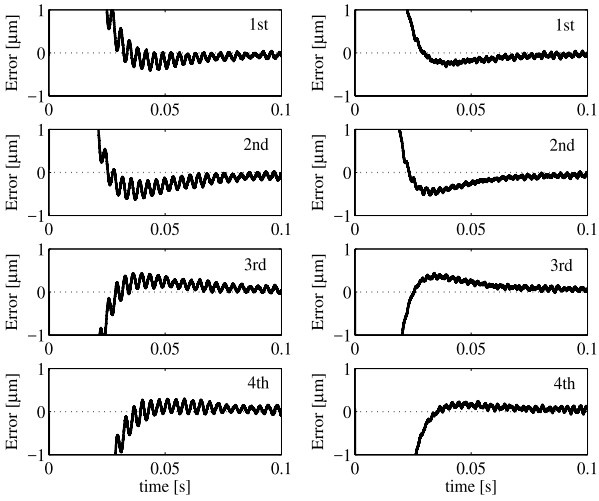

Fig. 14. Error waveforms for each step reference ($r-y$) in inching motion

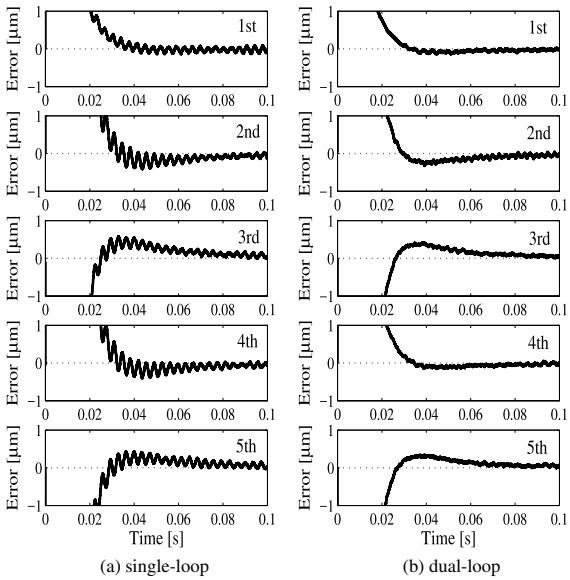

Fig. 15. Error waveforms for each step reference ($r-y$) in step motion with different amplitudes

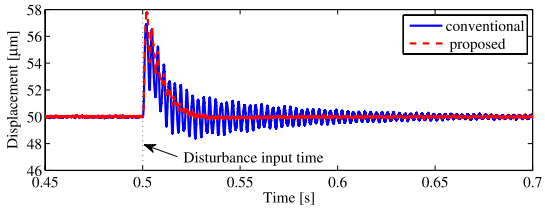

Fig. 16. Response waveforms for the impulse disturbance after positioning

mum amplitude of residual vibration after settling is approximately 30 [nm] for each response. To improve the convergence performance, optimal algorithm for parameter tuning considering robustness should be introduced. In addition, sensor performance, e.g. resolution and S/N ratio, should be improved.

Figure 16 shows the response waveforms for the impulse disturbance, where the disturbance is inputted at 0.5 [s] after positioning for 50 [μm]. This result shows that the disturbance can be suppressed sufficiently because the sensitivity gain at the resonant frequencies reduces by employing the minor-loop control system.

5. Conclusions

This paper presented a robust vibration suppression approach against resonant frequency variations in the piezo-actuated stage. In the proposed control system, dual-loop position controller was designed. The design of a minor-loop compensator focused on the reduction of sensitivity gain at around the resonant frequencies, where phase stabilization approach was introduced as a design guideline. On the other hand, a major-loop compensator was designed by considering system stability, servo bandwidth, and settling performance. The proposed design approach is clear design guideline and practical because the design parameters are only two. The proposed approach was verified by experiments using the piezo-actuated stage.

References

(1) T. Atsumi: “Emerging Technology for Head-Positioning System in HDDs”, *IEEJ Journal of IA*, Vol.5, No.2, pp.117–122 (2016)

(2) K. Yoshida, K. Ohishi, T. Miyazaki, Y. Yokokura, and J. Fukui: “Full FPGA Tracking Control System Based on Error-Based Communication Disturbance Observer Considering Time Delay for Optical Disc System”, *IEEJ Journal of IA*, Vol.6, No.2, pp.91–99 (2017)

(3) Y. Urakawa: “Lens Position Control System Using Limited Pole Placement Method”, *IEEJ Journal of IA*, Vol.6, No.2, pp.117–123 (2017)

(4) M.F. Heertjes: “Variable Gain Motion Control of Wafer Scanners”, *IEEJ Journal of IA*, Vol.5, No.2, pp.90–100 (2016)

(5) W. Ohnishi, H. Fujimoto, K. Sakata, K. Suzuki, and K. Saiki: “Decoupling Control Method for High-Precision Stages using Multiple Actuators considering the Misalignment among the Actuation Point, Center of Gravity, and Center of Rotation”, *IEEJ Journal of IA*, Vol.5, No.2, pp.141–147 (2016)

(6) E.J. Kim, K. Seki, M. Iwasaki, and S.H. Lee: “GA-Based Practical Auto-Tuning Technique for Industrial Robot Controller with System Identification”, *IEEJ Journal of Industry Applications*, Vol.1, No.1, pp.62–69 (2012)

(7) T. Yoshioka, A. Yabuki, Y. Yokokura, K. Ohishi, T. Miyazaki, and T.T. Phuong: “Stable Force Control of Industrial Robot Based on Spring Ratio and Instantaneous State Observer”, *IEEJ Journal of IA*, Vol.5, No.2, pp.132–140 (2016)

(8) K. Yu, T. Matsunaga, H. Kawana, S. Usuda, and K. Ohnishi: “Frequency-Based Analysis of the Relationship between Cutting Force and CT Number for an Implant-Surgery-Teaching Robot”, *IEEJ Journal of IA*, Vol.6, No.1, pp.66–72 (2017)

(9) S. Devasia, E. Eleftheriou and S.O. Reza Moheimani: “A Survey of Control Issues in Nanopositioning”, *IEEE Trans. on Control Systems Technology*, Vol.15, No.5, pp.802–823 (2007)

(10) M. Rakotondrabe: “Bouc-Wen Modeling and Inverse Multiplicative Structure to Compensate Hysteresis Nonlinearity in Piezoelectric Actuators”, *IEEE Trans. on Automation Science and Engineering*, Vol.8, No.2, pp.428–431 (2011)

(11) G. Song, J. Zhao, X. Zhou, and J. Alexis De Abreu-Garcia: “Tracking Control of a Piezoceramic Actuator With Hysteresis Compensation Using Inverse Preisach Model”, *IEEE/ASME Trans. on Mechatronics*, Vol.10, No.2, pp.198–209 (2005)

(12) M.A. Janaideh, S. Rakheja, and C.Y. Su: “An Analytical Generalized Prandtl-Ishlinskii Model Inversion for Hysteresis Compensation in Micropositioning Control”, *IEEE/ASME Trans. on Mechatronics*, Vol.16, No.4, pp.734–744 (2011)

(13) K.K. Leang and S. Devasia: “Feedback-Linearized Inverse Feedforward for Creep, Hysteresis, and Vibration Compensation in AFM Piezoactuators”, *IEEE Trans. on Control Systems Technology*, Vol.15, No.5, pp.927–935 (2007)

(14) M. Iwasaki, K. Seki, and Y. Maeda: “High Precision Motion Control Techniques—A Promissing Approach to Improving Motion Perfromance”, *IEEE Industrial Electronics Magazine*, Vol.6, No.1, pp.32–40 (2012)

(15) W. Xu and T. King: “Flexure hinges for piezoactuator displacement amplifiers: flexibility, accuracy, and stress considerations”, *Precision Engineering*, Vol.19, No.1, pp.4–10 (1996)

(16) Y. Okazaki: “A Micro-Positioning Tool Post Using a Piezoelectric Actuator for Diamond Turning Machines”, *Precision Engineering*, Vol.12, No.3, pp.151–156 (1990)

(17) K. Seki, M. Ruderman, and M. Iwasaki: “Modeling and Compensation for Hysteresis Properties in Piezoelectric Actuators”, *Proc. of 13th International Workshop on Advanced Motion Control*, pp.687–692 (2014)

(18) K.K. Leang, Q. Zou, and S. Devasia: “Feedforward Control of Piezoactuators in Atomic Force Microscope Systems: Inversion-Based Compensation for Dynamics and Hysteresis”, *IEEE Control Systems Magazine*, Vol.29, No.1, pp.70–82 (2009)

(19) M.W. Fairbairn, S.O.R. Moheimani, and A.J. Fleming: “Q-Control of an Atomic Force Microscope Microcantilever: A Sensorless Approach”, *IEEE/ASME Journal of Microelectromechanical Systems*, Vol.20, No.6, pp.1372–1381 (2011)

(20) K. Seki and M. Iwasaki: “Application of Self-sensing Technique for Position Control Considering Vibration Suppression in Piezo-driven Stage”, *Proc. of the 8th IEEE International Conference on Mechatronics*, pp.274–279 (2015)

(21) Y.K. Yong and A.J. Fleming: “High-speed Vertical Positioning Stage with Integrated Dual-sensor Arrangement”, *Sensors and Actuators A: Physical*, Vol.248, No.1, pp.184–192 (2016)

(22) J. Zhong and B. Yao: “Adaptive Robust Precision Motion Control of a Piezoelectric Positioning Stage”, *IEEE Trans. on Control Systems Technology*, Vol.16, No.5, pp.1039–1046 (2008)

(23) S. Salapaka, A. Sebastian, J.P. Cleveland, and M.V. Salapaka: “High bandwidth nano-positioner: A robust control approach”, *Review of Scientific Instruments*, Vol.73, No.9, pp.3232–3241 (2002)

(24) K. Abidi and A. Sabanovic: “Sliding-Mode Control for High-Precision Motion of a Piezostage”, *IEEE Trans. on Industrial Electronics*, Vol.54, No.1, pp.629–637 (2007)

(25) Y. Shan and K.K. Leang: “Design and Control for High-Speed Nanopositioning: Serial-Kinematic Nanopositioners and Repetitive Control for Nanofabrication”, *IEEE Control Systems Magazine*, Vol.33, No.6, pp.86–105 (2013)

(26) T. Atsumi, T. Arisaka, T. Shimizu, and H. Masuda: “Head Positioning Control Using Resonant Modes in Hard Disk Drives”, *IEEE/ASME Trans. on Mechatronics*, Vol.10, No.4, pp.378–384 (2005)

(27) W. Messner, M. Bedillion, L. Xia, and D. Karns: “Lead and Lag Compensators with Complex Poles and Zeros: design formulas for modeling and loop shaping”, *IEEE Control Systems Magazine*, Vol.27, No.1, pp.44–54 (2007)

Kenta Seki (Senior Member) received the B.S., M.S., and Dr.Eng. degrees in electrical and computer engineering from Nagoya Institute of Technology, Nagoya, Japan, in 2000, 2002 and 2009, respectively. From 2002 to 2006, he was with the Mechanical Engineering Research Laboratory, Hitachi, Ltd., Ibaraki, Japan. From March 2006, he joined a Research Associate with the Project Research Laboratory on Motion Systems, Nagoya Institute of Technology, Nagoya, Japan, where he is currently an Associate Professor with the Department of Electrical and Mechanical Engineering. His current research interests are the mechatronics system design and design of dynamically testing systems.

Daisuke Noda (Member) received the B.S. degree in electrical and electronic engineering from Nagoya Institute of Technology, Nagoya, Japan, in 2014. Since 2014, he has been a Master's course at Nagoya Institute of Technology, Nagoya, Japan. His research interests are the high precision motion controller design.

Makoto Iwasaki (Senior Member) received the B.S., M.S., and Dr.Eng. degrees in electrical and computer engineering from Nagoya Institute of Technology, Nagoya, Japan, in 1986, 1988, and 1991, respectively. Since 1991, he has been with the Department of Computer Science and Engineering, Nagoya Institute of Technology, where he is currently a Professor. His current research interests are the applications of control theories to linear/nonlinear modeling and precision positioning, through various collaborative research activities with industries.